# Fbw7 controls neural stem cell differentiation and progenitor apoptosis via Notch and c-Jun

Joerg D Hoeck, Anett Jandke, Sophia Maria Blake, Emma Nye, Bradley Spencer-Dene, Sebastian Brandner, Axel Behrens

**Fbw7 controls neural stem cell differentiation and progenitor apoptosis via Notch and c-Jun**

Joerg D Hoeck[1], Anett Jandke[1], Sophia M Blake[1], Emma Nye[2], Bradley Spencer-Dene[2], Sebastian Brandner[3] and Axel Behrens[1, 4]

[1] Mammalian Genetics Laboratory
[2] Experimental Pathology Laboratory
Cancer Research UK London Research Institute
Lincoln's Inn Fields Laboratories
44 Lincoln's Inn Fields
London WC2A 3LY
United Kingdom

[3]Division of Neuropathology, Department of Neurodegenerative Disease, Institute of Neurology, London, UK

[4] Address correspondence to
Axel Behrens
Tel: 44-207-269 3361
Fax: 44-207-269 3093
Email: axel.behrens@cancer.org.uk

Key words: Fbw7, c-Jun, Notch, ubiquitylation, E3 ligase, neural stem cell

**ABSTRACT**

**Neural stem/progenitor cells (NSCs/NPCs) give rise to neurons, astrocytes, and oligodendrocytes. However, the mechanisms underlying the decision of a stem cell to either self-renew or differentiate are incompletely understood. We demonstrate here that Fbw7 (F-box and WD repeat domain containing 7), the substrate recognition component of an SCF (complex of SKP1, CUL1 and F-box protein)-type E3 ubiquitin ligase, is a key regulator of murine NSC/NPC viability and differentiation. The absence of Fbw7 caused severely impaired stem cell differentiation and increased progenitor cell death. Fbw7 deficiency resulted in accumulation of the SCF(Fbw7) substrates active Notch1 and N-terminally phosphorylated c-Jun. Genetic and pharmacological rescue experiments identified c-Jun as a key substrate of Fbw7 in controlling progenitor cell viability, whereas inhibition of Notch signalling alleviated the block in stem cell differentiation. Thus Fbw7 controls neurogenesis by antagonising Notch and JNK/c-Jun signalling.**

## INTRODUCTION

Neural stem cells (NSCs) produce the differentiated cell types of the nervous system, namely neurons and glia. The first NSCs to appear during embryogenesis are neuroepithelial cells. Subsequently, other stem cell populations arise, i.e. radial glia cells (RGCs) at later stages of embryonic development and stem cells with astroglial characteristics in the adult[1,2]. NSCs have been suggested as a potential therapeutic tool for neurodegenerative diseases and neural injuries. However, a pre-requisite to manipulate stem cell behaviour is to better understand the mechanisms that govern NSC homeostasis and differentiation.

Fbw7 (also known as Fbxw7, hCdc4, hSel-10) is a member of the F-box family of proteins, which function as substrate recognition adaptors for SCF (complex of SKP1, CUL1 and F-box protein)-type ubiquitin ligases[3]. SCF(Fbw7) targets several important oncoproteins, including c-Myc, c-Jun, CyclinE1 and Notch, for ubiquitin-dependent proteolysis and Fbw7 mutations have been detected in a variety of human cancers, indicating that Fbw7 is a tumour suppressor[4–6].

Several Fbw7 substrates have been implicated in the control of neural differentiation and viability. The AP-1 transcription factor c-Jun is an important regulator of neuronal viability, especially when phosphorylated by the JNK group of MAP kinases[7–9]. The Notch signalling pathway controls neural differentiation and is known to maintain NSC character and to inhibit neurogenesis. The Notch-Hes pathway is necessary for self-renewing cell division and thus, maintenance of the neural precursor population[10–13]. However, the significance of the regulation of c-Jun, Notch and other substrates by SCF(Fbw7) during neurogenesis has remained unclear to date. In this study we identify the E3 ubiquitin ligase Fbw7 as a key regulator of neural stem cell differentiation and progenitor viability. We demonstrate that Fbw7 acts as a molecular switch that antagonises Notch activity and JNK/c-Jun signalling to enable neural stem cell differentiation and progenitor survival.

## RESULTS

### Conditional inactivation of Fbw7 in the nervous system

To investigate the significance of Fbw7 expression and function during neural development, we generated conditional knock-out mice in which exon 5 of *fbw7* was flanked by loxP sites (**Supplementary Fig. 1a**), since mice lacking Fbw7 die during early embryonic development due to placental and vascular defects[14,15]. Deletion of exon 5 removes most of the F-box, an essential domain of Fbw7, and in addition disrupts the *fbw7* open reading frame preventing production of detectable Fbw7 protein (Jandke *et al. in preparation*, and below).

Floxed *fbw7* (*fbw7*$^{f/f}$) mice were crossed to Nestin-Cre transgenic mice previously shown to provide efficient NSC-specific Cre activity[9], with no recombination detectable in neural crest-derived cells[16]. *In situ* hybridisation revealed loss of *fbw7* expression in *fbw7*$^{f/f}$; Nestin-Cre$^{+}$ mutant mice (*fbw7*$^{\Delta N}$ mice) confirming efficient Cre-mediated deletion (**Supplementary Fig. 1b**). *fbw7*$^{\Delta N}$ mice were not obtained at weaning age and died perinatally (data not shown).

### Fbw7 controls cell number and differentiation in the brain

While the overall structure of *fbw7*$^{\Delta N}$ mutant brains was normal, histological analysis of E18.5 mutant embryos revealed severe defects in neurogenesis. The size and thickness of brain regions such as the cortex was unaffected by the absence of Fbw7 (**Supplementary Fig. 2**), whereas the cellularity in several regions of the developing *fbw7*$^{\Delta N}$ brain was significantly reduced. In the E18.5 midbrain tectum and forebrain cortex, cell numbers were decreased by around 30% in areas where committed progenitors and differentiated cells reside, namely the tectal mantle layer (ML) as well as the cortical subventricular zone (SVZ), intermediate zone (IZ) and cortical plate (CP) (**Fig. 1a**–**d**). Similarly, the cellularity in *fbw7*$^{\Delta N}$ embryos was decreased in other brain regions such as the cerebellar anlage and the thalamus (**Supplementary Fig. 3**). In contrast, the cellularity in compartments harbouring immature cells was either unaffected, as in the cortical ventricular zone (VZ), or increased, as seen in

the tectal VZ (**Fig. 1a**–**d**). Whilst we could not detect a statistically significant difference in the number of proliferating cells (**Fig. 1e**,**g**), the number of apoptotic cells marked by active Caspase 3 was significantly increased in the tectal ML at E16.5 (**Fig. 1f**,**g**).

To better understand the role of Fbw7 during brain development, we performed *in situ* hybridisation for *fbw7* and immunohistochemistry (IHC) for markers characterising neural stem cells, progenitors and differentiated cells. *fbw7* mRNA was highly expressed at E14.5 in the cortical VZ and SVZ, indicating a role for Fbw7 in stem cells and progenitors (**Fig. 2a**). Expression of the neural stem cell and progenitor marker Nestin was already slightly increased in the E14.5 cortex of *fbw7*$^{\Delta N}$ mice. At E16.5 and E18.5, this difference in Nestin expression was more pronounced (**Fig. 2b**–**d**). The overall number of proliferating cells in the SVZ was not affected at various stages of development (**Supplementary Fig. 4**). Immunoreactivity for the radial glia markers glutamate aspartate transporter (GLAST) and Brain lipid binding protein (BLBP) was augmented (**Fig. 2c**,**e**,**f**). Indeed, quantification revealed a significant increase in BLBP-positive cells in the SVZ of the *fbw7*$^{\Delta N}$ E18.5 cortex (**Fig. 2l**). In contrast, the abundance of intermediate progenitor cells marked by Tbr2 was diminished in the mutant cortex (**Fig. 2g**,**l**). Besides the decrease in Tbr2-positive intermediate progenitors, the proportion of Doublecortin-positive neuronal progenitors was reduced in the mutant SVZ throughout embryonic brain development (**Supplementary Fig. 5**). Consequently the number of cells expressing markers for neurons, NeuN, Tbr1, Ctip2 and Brn2, was decreased to varying extent (**Fig. 2h**–**l**). Since there is a substantial reduction in total cell number in areas of differentiated cells (**Fig. 1a**,**c**) and a reduced percentage of neurons, the absolute number of neurons is reduced by more than 50% in the *fbw7*$^{\Delta N}$ cortex. In contrast to neurogenesis, absence of *fbw7* did not have a significant effect on gliogenesis. GFAP-positive cells were hardly detectable in the IZ and CP of both the control and the mutant cortex at E18.5 and there was no significant difference in the number of cells expressing the astroglia marker S100 (**Supplementary Fig. 6a**–**c**). There was also no change

in the percentage of cells expressing the oligodendroglia marker NG2 (**Supplementary Fig. 6d**,**e**). Similar to the cortex, an accumulation of cells expressing markers of immature cells and a reduction in NeuN-positive cells was also seen in the *fbw7*$^{\Delta N}$ tectum (**Supplementary Fig. 7**). It is likely that the severe reduction of neurons in *fbw7*$^{\Delta N}$ brains contributes to the perinatal lethality.

**Fbw7 controls neurosphere cell survival and differentiation**

To further investigate the function of Fbw7 in NSCs/NPCs, we prepared neurosphere cultures from E14.5 embryos. Neurospheres consist predominantly of neural progenitors and to a small extent of stem cells and differentiated cells[18]. Neurospheres derived from *fbw7*$^{\Delta N}$ embryos were on average smaller in size and the number of neurospheres was significantly decreased (**Fig. 3a**–**c**). The loss of Fbw7 function had no significant effect on NSC/NPC proliferation analysed by staining for pH3 and CFSE dilution (**Supplementary Fig. 8**). Whilst the large majority of cells in both control and *fbw7*$^{\Delta N}$ neurospheres expressed Nestin, the percentage of cells positive for Musashi-1 (Msi-1), which marks more immature cells, was greatly increased in *fbw7*$^{\Delta N}$ neurospheres (**Fig. 3d**,**e**). Similar to our observations in the cortex, the number of neurosphere cells expressing glial markers was not significantly altered in the absence of Fbw7 (**Supplementary Fig. 6f**–**i**). Moreover, TUNEL assay revealed substantially increased cell death in *fbw7*$^{\Delta N}$ neurospheres (**Fig. 3f**,**g**). Thus it appears that a decrease in cell differentiation, accompanied by excessive progenitor cell death, reduces the efficiency of *fbw7*$^{\Delta N}$ neurosphere formation. This predicts that the rescue of cell death would improve neurosphere formation, an experiment we describe below.

We next investigated the differentiation potential of Fbw7-deficient NSCs/NPCs. Cultured NSCs/NPCs from control mice readily formed a monolayer of cells after induction of differentiation, but *fbw7*$^{\Delta N}$ mutant NSCs/NPCs often retained the ball-shaped neurosphere

morphology (**Supplementary Fig. 9**), indicative of a problem to undergo the differentiation programme. 5 days after the onset of differentiation, the percentage of Nestin-positive NSCs/NPCs was low in control cultures. In contrast, a higher number of *fbw7*$^{\Delta N}$ neural cells retained Nestin expression (**Fig. 4a**,**d**). To further characterise the Nestin-positive cells that accumulated in *fbw7*$^{\Delta N}$ differentiation cultures, we investigated the expression of the classical RGC marker RC2. The majority of Nestin-positive cells were also RC2-positive (**Fig. 4a**,**d**), and the absence of Fbw7 also led to increased numbers of cells expressing two further RGC markers, BLBP and Vimentin (**Supplementary Fig. 10a**), indicating that RGCs represent the main immature cell population accumulating in *fbw7*$^{\Delta N}$ differentiation cultures. Additionally, CD133-positive neuroepithelial stem cells were very rare in control cultures 5 days after the onset of differentiation, whereas in *fbw7*-deficient cultures CD133-positive cells were readily detectable (**Supplementary Fig. 10b**). A similar increase in Nestin-positive cells was also observed when adherent NSC cultures were induced to differentiate (**Supplementary Fig. 11a**–**d**). The accumulation of immature neural cells in *fbw7*$^{\Delta N}$ neurosphere cultures was also observed after prolonged time (11 days) under differentiation conditions, indicating that Fbw7 inactivation does not only delay, but genuinely blocks efficient neural differentiation (**Supplementary Fig. 12**). Conversely, the percentage of differentiated cells expressing the neuronal marker Map2 was reduced (**Fig. 4b**,**d**) whereas the frequency of astrocytes expressing Connexin43 and oligodendrocytes marked by O4 were not significantly altered in mutant differentiation cultures (**Fig. 4b**–**d**). Triple IF staining revealed that the vast majority of both control and *fbw7*$^{\Delta N}$ neurospheres gave rise to differentiated cells of all 3 lineages (**Supplementary Fig. 13**). Taken together, the absence of Fbw7 results in decreased neurogenesis and an accumulation of cells expressing radial glia markers in cultured neurospheres.

**Fbw7 antagonises c-Jun to regulate neural cell viability**

The *fbw7* locus encodes 3 different Fbw7 isoforms which are generated by alternative splicing of the first exon[4]. Whereas the α and β *fbw7* splice variants were expressed in neurospheres, the γ isoform was undetectable. *fbw7* α and β were also present in total adult brain RNA. Notably, other organs showed different *fbw7* splicing patterns (**Supplementary Fig. 14**). Fbw7 protein was detected in control neurosphere extracts but was absent in $fbw7^{\Delta N}$ neurospheres (**Fig. 5a**). To understand the mechanism of Fbw7 function, we investigated the expression levels of known substrates of SCF(Fbw7). Whilst phosphorylated c-Myc and phosphorylated CyclinE protein levels were not substantially altered, there was a significant increase in the levels of active Notch1 and phosphorylated c-Jun (**Fig. 5a** and **Supplementary Fig. 11e**).

Phosphorylated c-Jun is an important regulator of neuronal viability[7–9], and we have previously demonstrated that depletion of Fbw7 leads to cell death in PC12 neuronal-like cells due to increased levels of phosphorylated c-Jun[19]. Thus we investigated whether increased c-Jun function contributed to cell death in the absence of Fbw7 during neurogenesis. As in neurosphere cultures, the expression level of phosphorylated c-Jun was also greatly increased in the brains of E18.5 $fbw7^{\Delta N}$ mutant embryos (**Fig. 5b**). To assess the functional importance of c-Jun downstream of Fbw7, one allele of the *c-jun* gene was inactivated in a $fbw7^{\Delta N}$-mutant background ($fbw7^{f/f}$; $c\text{-}jun^{f/+}$; Nestin-$Cre^{+}$ or $fbw7^{\Delta N}$; $c\text{-}jun^{\Delta N/+}$ mutant mice). Heterozygous deletion markedly reduced the levels of phosphorylated c-Jun in the brain of Fbw7-deficient embryos (**Fig. 5b**). Genetic reduction of c-Jun function significantly rescued the defect in cellularity in the mantle layer of the midbrain tectum, but the number of stem cells in the tectal ventricular zone was still elevated in $fbw7^{\Delta N}$; $c\text{-}jun^{\Delta N/+}$ embryos (**Fig. 5c** and **Supplementary Fig. 16**). Likewise, neurosphere formation *in vitro* was substantially increased in $fbw7^{\Delta N}$; $c\text{-}jun^{\Delta N/+}$ cells compared to $fbw7^{\Delta N}$ single mutants, which was accompanied by a considerable reduction in TUNEL-positive apoptotic cells in $fbw7^{\Delta N}$; *c-*

*jun*$^{\Delta N/+}$ neurospheres (**Fig. 5d**,**e**), indicating that c-Jun-mediated cell death is causally involved in defective *fbw7*$^{\Delta N}$ neurosphere formation.

An important mechanism of c-Jun-mediated control of neuronal viability is the transcriptional regulation of pro-apoptotic members of the Bcl2 family of proteins[20–22]. mRNA levels of *c-jun*, which is autoregulated by the c-Jun protein itself[23], were increased in the absence of Fbw7. Likewise, the expression of the pro-apoptotic genes *bad* and *bim* were augmented to varying extents. The expression of the anti-apoptotic *bcl2* gene was unaffected (**Fig. 5f**). As cells with the highest levels of phosphorylated c-Jun are expected to undergo apoptosis in neurosphere cultures, it is plausible that this analysis underestimates the effect of Fbw7 inactivation on c-Jun-mediated gene activation. Heterozygosity for *c-jun* reduced the expression of the pro-apoptotic c-Jun target genes (**Fig. 5f**). In summary, negative regulation of c-Jun activity by Fbw7 is essential to prevent excessive cell death during neurogenesis. Thus downregulation of c-Jun in the *fbw7*$^{\Delta N}$ background rescued neurosphere formation and the number of apoptotic neurosphere cells *in vitro* and the reduction in cell number *in vivo*.

**Fbw7 antagonises Notch to allow NSC differentiation**

Heterozygosity for *c-jun* did not rescue the differentiation defect and the increased number of cells with radial glia identity in differentiating *fbw7*$^{\Delta N}$ neurosphere cultures, arguing that c-Jun protein levels are not critical for Fbw7-regulated neural differentiation (**Supplementary Fig. 17**). In contrast, deregulated Notch signalling was a possible candidate for the differentiation defects observed in *fbw7*$^{\Delta N}$ mutants *in vivo* and *in vitro*. Overexpression of the activating intracellular fragment of Notch1, the NICD1, has been shown to be sufficient to promote radial glia identity during embryogenesis while abrogation of Notch signalling leads to depletion of RGCs[10,24]. However, the molecular mechanism that antagonises Notch activity to allow neural differentiation to occur is not known.

The increased protein expression of NICD1 seen by immunoblotting was confirmed by IHC

(**Fig. 6a**), indicating that Fbw7 regulates NICD1 levels both *in vitro* and *in vivo*. Our observation that BLBP levels were higher in *fbw7*$^{\Delta N}$ mutant embryos and neurosphere cultures (**Fig. 2c**,**f**,**l** and **Supplementary Figs. 7** and **10a**) was a first indication that increased Notch immunoreactivity translated into increased Notch function, since BLBP was reported to be a direct target of the Notch signalling pathway[25].

To address the functional significance of increased Notch activity in Fbw7-regulated neural differentiation, we performed genetic and pharmacological rescue experiments. One allele of the *Notch1* gene[26] was inactivated in a *fbw7*$^{\Delta N}$-mutant background (*fbw7*$^{f/f}$; *Notch1*$^{\Delta/+}$; Nestin-Cre$^{+}$ or *fbw7*$^{\Delta N}$; *Notch1*$^{\Delta/+}$ mutant mice). In addition, we made use of the γ-secretase inhibitor N-[N-(3,5-Difluorophenacetyl-L-Alanyl)]-S-phenylglycine t-butyl ester (DAPT), which prevents the release of the activating intracellular fragment of Notch proteins[27]. The deletion of one *Notch1* allele in the *fbw7*$^{\Delta N}$ background reduced the levels of NICD1 (**Fig. 6a**). *Notch1* heterozygosity attenuated the accumulation of BLBP-positive cells and Nestin immunoreactivity and partially rescued the number of NeuN-positive neurons in the *fbw7*$^{\Delta N}$-mutant cortex (**Fig. 6b**–**d** and **Supplementary Fig. 18a**,**b**). mRNA levels of the classical Notch target genes *hes5* and *hey1* were augmented in *fbw7*$^{\Delta N}$ neurosphere cultures, whereas *hes1* levels were not significantly altered (**Fig. 6e** and **Supplementary Figs. 11f** and **19a**). Heterozygosity for *Notch1* as well as DAPT treatment resulted in a significant reduction in the expression of *hes5* and *hey1* (**Fig. 6e** and **Supplementary Fig. 19a**).

Consequently, we next determined whether aberrant Notch activity contributes to the differentiation defects in *fbw7*$^{\Delta N}$ neurosphere cultures. Both *Notch1* heterozygosity or DAPT treatment resulted in a substantial reduction in the percentage of Nestin-positive cells in *fbw7*$^{\Delta N}$ mutant differentiation cultures and the number of Map2-positive neurons was significantly increased in *fbw7*$^{\Delta N}$; *Notch1*$^{\Delta/+}$ in comparison to *fbw7*$^{\Delta N}$ cultures (**Fig. 6f**,**g** and **Supplementary Figs. 18c**,**d** and **19b**,**c**). This suggests that Fbw7 is essential to antagonise

Notch signalling to allow neural differentiation to occur.

## DISCUSSION

This study identifies Fbw7 as a key regulator of neural progenitor viability and neural stem cell differentiation. We detected increased immunoreactivity for Nestin, GLAST and BLBP in the *fbw7*-mutant brain, suggesting that Fbw7 deficiency increases the number of immature cells. It is worth noting that GLAST and BLBP are also expressed in some astrocytes postnatally[2,28]. Thus it was possible that the supernumerary GLAST-positive and BLBP-positive cells in the *fbw7*$^{\Delta N}$ cortex were generated due to an increase in astrogliogenesis. However, expression of the astrocyte markers GFAP, S100 and Connexin43 was unaltered in *fbw7*-mutant cells (**Fig. 4b**,**d** and **Supplementary Fig. 6a**–**c**,**f**,**g**). The increased percentage of cells positive for RC2 and other RGC markers in differentiating neurospheres (**Fig. 4a**,**d** and **Supplementary Fig. 10a**) together with the known function of Notch signalling to promote RGC fate[24,29] is in agreement with a role for Fbw7 in RGC development.

While we have obtained no evidence for a defect in gliogenesis, Fbw7 deficiency leads to decreased numbers of neurons (**Fig. 2h**–**l**). The loss of Fbw7 led to a reduction of Tbr2-positive intermediate progenitors (**Fig. 2g**,**l**). There was also a significant decrease in Doublecortin-positive neuroblasts in the mutant SVZ throughout embryonic brain development, indicative of a defect in neurogenesis (**Supplementary Fig. 5**). It is conceivable that Fbw7 deficiency inhibits neural stem cell differentiation at the expense of neuronal progenitors, a phenotype consistent with a gain of Notch function[24]. Furthermore, Fbw7 deficiency increases progenitor cell death, which leads to a further reduction in neuronal number. However, a defect in neuronal maturation, and thus marker expression, may also contribute to the *fbw7*$^{\Delta N}$ phenotype.

SCF(Fbw7) has several substrates with diverse biological activities. Downregulation of the Fbw7-substrate c-Jun in the *fbw7*$^{\Delta N}$ background rescued the increased number of apoptotic neurosphere cells and the reduced number of cells in areas of differentiated cells in the brain. Regulation of c-Jun by Fbw7 is essential to control neural cell viability. Paradoxically, JNK activity is very high in neurons[19,30], and a role for JNK signalling in neuronal migration and maintenance of cytoskeletal integrity of neuronal cells has been described[31,32]. Therefore SCF(Fbw7) may function to inactivate apoptotic c-Jun-dependent JNK signalling, allowing neural cells to tolerate potentially neurotoxic JNK activity.

c-Jun is not involved in the regulation of neural differentiation by Fbw7. This process is controlled by Fbw7 through the regulation of Notch activity. Downregulation of the Fbw7-substrate Notch in the *fbw7*$^{\Delta N}$ background alleviated the block in cell differentiation and rescued neuronal numbers. While it is known that Notch activity needs to be downregulated for neuronal differentiation to occur[12], the mechanism that controls this transition has remained enigmatic. This work shows for the first time that Fbw7 is an important molecular switch that is required for attenuation of Notch activity during neurogenesis. It is noteworthy that SCF(Fbw7) can target various members of the Notch family of proteins[14], making it well-suited as a general antagonist of Notch function. Decreased Notch pathway activity in mice lacking *Notch1*, *rbp-j* (*cbf1*) or the Notch ligand *dll1* as well as in *hes1* single and *hes1*/*hes5* double mutants results in precocious neuronal differentiation[12,13]. *hes5* and *hes1* are well known targets of the Notch signalling pathway[33], and are crucial mediators of Notch function in the brain. However, in many instances *hes1* and *hes5* are differentially regulated. Notch-1 or RBP-J-mutant embryos show reduced expression of *hes5*, but *hes1* expression was normal[13,34]. Similarly, γ-secretase inhibition of Notch activity in neural progenitors was reported to have a much stronger effect on *hes5* compared to *hes1*[35]. In our mouse model *fbw7* deletion induces *hes5* mRNA increase while having a mild effect on *hes1,* suggesting that *fbw7* affects Notch1 with an overall balance towards *hes5*. This is in line with previous

observations in the mouse retina, in which glial cell specification is modulated by *hes5* in a *hes1*-independent manner[36].

Fbw7 appears to use distinct substrates to regulate different biological processes, however the molecular mechanism of how this occurs remains unknown. For instance, c-Myc protein accumulates in *fbw7*-deficient hematopoietic stem cells[37]. In contrast, Notch1 and c-Jun are increased upon *fbw7* deletion in mouse embryonic fibroblasts (MEFs), but no effect is found on CyclinE or c-Myc in these cells[38]. In the developing brain, the main SCF(Fbw7) substrates affected are Notch1 and c-Jun, while c-Myc and CyclinE protein levels are not greatly altered. One potential explanation could be the relative abundance of Fbw7 isoforms. The Fbw7γ isoform has been shown to mediate degradation of c-Myc and CyclinE[39–41]. The absence of Fbw7γ in neural stem cells and progenitors (**Supplementary Fig. 14**) could therefore impede efficient degradation of CyclinE or c-Myc. Thus differential expression of Fbw7 isoforms may contribute to cell-type specific substrate degradation.

The function of Fbw7 in stem cells is highly dependent on the organ system. Whereas we demonstrate here that Fbw7 is required for neural differentiation, inactivation of Fbw7 in hematopoietic stem cells (HSCs) causes defective maintenance of quiescence and premature depletion of HSCs[37,42]. Thus the lack of Fbw7 leads to opposite functional consequences in HSCs and NSCs. It is plausible that cell-type specific differential regulation of Fbw7 and its substrates is one mechanism that could explain the distinct roles of Fbw7 in different types of stem cells.

**FIGURE LEGENDS**

**Figure 1** Fbw7 controls cell number and survival in the brain. (**a**) Haematoxylin and eosin (H&E) staining of the E18.5 forebrain from *fbw7*$^{f/f}$ and *fbw7*$^{\Delta N}$ mouse embryos. Rectangles mark comparable regions of the cortex shown below in high magnification. Scale bars: 100 µm. (**b**) H&E staining of comparable regions of the *fbw7*$^{f/f}$ and *fbw7*$^{\Delta N}$ E18.5 midbrain. Rectangles mark the area of the tectum shown below in high magnification. Scale bars: 200 µm. (**c**) Histogram showing the relative quantity of cells in the ventricular zone (VZ), subventricular zone (SVZ), intermediate zone (IZ) and the cortical plate (CP) of the *fbw7*$^{f/f}$ and *fbw7*$^{\Delta N}$ E18.5 cortex. Cell number in the *fbw7*$^{f/f}$ E18.5 cortex is normalised to 1 (= 100%); n = 3. (**d**) Histogram showing the relative quantity of cells in the ventricular zone (VZ) and the mantle layer (ML) of the *fbw7*$^{f/f}$ and *fbw7*$^{\Delta N}$ E18.5 tectum. Cell numbers in the *fbw7*$^{f/f}$ E18.5 tectum are normalised to 1 (= 100%); n = 5. (**e**) 3,3'-Diaminobenzidine (DAB) staining for the mitotic marker phosphorylated histone H3 (pH3) on representative sections of the *fbw7*$^{f/f}$ and *fbw7*$^{\Delta N}$ E16.5 tectum. Cells are counterstained with H&E. Scale bars: 50 µm. (**f**) Immunohistochemistry for active Caspase 3 (Casp3; green) on representative sections of the *fbw7*$^{f/f}$ and *fbw7*$^{\Delta N}$ E16.5 tectum. DNA (blue) is counterstained with DAPI. Scale bars: 50 µm. (**g**) Quantification of phosphorylated histone H3 (pH3$^{+}$) and active Caspase 3 (Casp3$^{+}$) positive cells in the *fbw7*$^{f/f}$ and *fbw7*$^{\Delta N}$ E16.5 tectum; n = 3.

Error bars represent the standard error of the mean (s.e.m.). Statistical significance: n.s.: not significant; *: $p \leq 0.05$; **: $p \leq 0.01$; ***: $p \leq 0.001$ (unpaired *t* test).

**Figure 2** Fbw7 controls stem cell differentiation and neurogenesis in the brain. (**a**) *fbw7* (exon 6–10 specific probe) *in situ* hybridisation and sense control with H&E counterstain on the *fbw7*$^{f/f}$ E14.5 cortex. Scale bars: 50 µm. (**b**) Immunohistochemistry for Nestin (red) on the

*fbw7*$^{f/f}$ and *fbw7*$^{\Delta N}$ E14.5 cortex. White rectangles mark areas shown in high magnification in panels at the top. DNA (blue) is counterstained with DAPI. Scale bars: 50 µm. (**c**) Immunohistochemistry for Nestin (red; left panels) and BLBP (red; right panels) on the *fbw7*$^{f/f}$ and *fbw7*$^{\Delta N}$ E16.5 cortex. White rectangles mark areas shown in high magnification in panels at the top. DNA (blue) is counterstained with DAPI. Scale bars: 50 µm. (**d**) DAB staining for Nestin on the *fbw7*$^{f/f}$ and *fbw7*$^{\Delta N}$ E18.5 cortex. Black rectangles mark areas shown in high magnification in panels at the top. Cells are counterstained with H&E. Scale bars: 50 µm. (**e**) Immunohistochemistry for GLAST (green) on the *fbw7*$^{f/f}$ and *fbw7*$^{\Delta N}$ E18.5 cortex. White rectangles mark areas shown in high magnification in panels at the top. Cells are counterstained with DAPI. Scale bars: 50 µm. DAB staining for (**f**) BLBP, (**g**) Tbr2**,** (**h**) NeuN**,** (**i**) Tbr1**,** (**j**) Ctip2 and (**k**) Brn2 on the *fbw7*$^{f/f}$ and *fbw7*$^{\Delta N}$ E18.5 cortex. Black rectangles mark areas shown in high magnification in panels at the top. Cells are counterstained with H&E. Scale bars: 50 µm. (**l**) Quantification of BLBP-positive cells in the SVZ and Tbr2, NeuN, Tbr1, Ctip2 and Brn2-positive cells in the IZ and the CP of the *fbw7*$^{f/f}$ and *fbw7*$^{\Delta N}$ E18.5 cortex. n = 3.

Error bars represent the s.e.m. Statistical significance: *: $p \leq 0.05$ (unpaired *t* test); **: $p \leq 0.01$. CP: cortical plate, IZ: intermediate zone, SVZ: subventricular zone, VZ: ventricular zone.

**Figure 3** Absence of Fbw7 leads to retention of markers for immature cells and induces apoptosis *in vitro*. (**a**) Phase contrast pictures of *fbw7*$^{f/f}$ and *fbw7*$^{\Delta N}$ neurosphere cultures under self-renewal conditions. Arrowheads denote neurospheres. Scale bars: 100 µm. Histograms showing (**b**) the size (in µm) and (**c**) the relative quantity of *fbw7*$^{f/f}$ and *fbw7*$^{\Delta N}$ neurospheres. Neurosphere numbers in *fbw7*$^{f/f}$ cultures are normalised to 1 (= 100%); n = 4. (**d**) Immunocytochemistry for Nestin (green)/Musashi1 (Msi1; red) on *fbw7*$^{f/f}$ and *fbw7*$^{\Delta N}$

neurosphere sections. DNA (blue) was counterstained with DAPI. Scale bars: 100 µm. (**e**) Quantification of Musashi1-positive cells ($Msi1^{+}$) per neurosphere in *fbw7*$^{f/f}$ and *fbw7*$^{\Delta N}$ neurosphere cultures; n = 3. (**f**) DAB staining for TUNEL (TdT-mediated dUTP-biotin nick end labeling) positive cells on *fbw7*$^{f/f}$ and *fbw7*$^{\Delta N}$ neurosphere sections. Arrowheads denote TUNEL-positive cells. Scale bars: 100 µm. (**g**) Histogram showing the percentage of TUNEL-positive cells in *fbw7*$^{f/f}$ and *fbw7*$^{\Delta N}$ neurosphere cultures; n = 3.

Error bars represent the s.e.m. Statistical significance: **: $p \leq 0.01$; ***: $p \leq 0.001$ (unpaired *t* test).

**Figure 4** Absence of Fbw7 blocks differentiation *in vitro*. Immunocytochemistry for (**a**) RC2 (green) and Nestin (red), (**b**) Map2 (green) and Connexin43 (Cx43; red) and (**c**) O4 on *fbw7*$^{f/f}$ and *fbw7*$^{\Delta N}$ neurosphere cultures after 5 days under differentiation conditions. White squares mark areas shown in high magnification in panels on the right. DNA (blue) was counterstained with Hoechst 33342. Scale bars: 50 µm. (**d**) Quantification of RC2/Nestin, Map2, Cx43 and O4-positive cells in *fbw7*$^{f/f}$ and *fbw7*$^{\Delta N}$ neurosphere cultures after 5 days under differentiation conditions.

Error bars represent the s.e.m. Statistical significance: n.s.: not significant; *: $p \leq 0.05$ (unpaired *t* test).

**Figure 5** Negative regulation of c-Jun by Fbw7 controls neural cell viability. (**a**) Western blot analysis of Fbw7, c-Jun, activated Notch1 (NICD1), threonine 58/serine 62 phosphorylated c-Myc (p-c-Myc), threonine 395 phosphorylated cyclinE and β-Actin on protein lysates from *fbw7*$^{f/f}$ and *fbw7*$^{\Delta N}$ neurospheres (cropped images, full-length blots are presented in **Supplementary Fig. 15a**). (**b**) Immunohistochemistry for serine 73 phosphorylated c-Jun (p-c-Jun; red) on representative sections of the *fbw7*$^{f/f}$, *fbw7*$^{\Delta N}$ and *fbw7*$^{\Delta N}$; *c-jun*$^{\Delta N/+}$ E18.5

tectum. DNA (blue) was counterstained with DAPI. Scale bars: 50 μm. (**c**) Histogram showing the relative quantity of cells in the ventricular zone (VZ) and the mantle layer (ML) of the *fbw7*$^{f/f}$ (n = 5), *fbw7*$^{\Delta N}$ (n = 5) and *fbw7*$^{\Delta N}$; *c-jun*$^{\Delta N/+}$ (n = 3) E18.5 tectum. Cell numbers in the *fbw7*$^{f/f}$ E18.5 tectum are normalised to 1 (= 100%). (**d**) Histogram showing the relative quantity of neurospheres in *fbw7*$^{f/f}$ (n = 4), *fbw7*$^{\Delta N}$ (n = 4) and *fbw7*$^{\Delta N}$; *c-jun*$^{\Delta N/+}$ (n = 2) neurosphere cultures after 2 weeks under self-renewal conditions. Neurosphere number in *fbw7*$^{f/f}$ neurosphere cultures are normalised to 1 (= 100%). (**e**) Histogram showing the percentage of TUNEL-positive cells in *fbw7*$^{f/f}$ (n = 3), *fbw7*$^{\Delta N}$ (n = 3) and *fbw7*$^{\Delta N}$; *c-jun*$^{\Delta N/+}$ (n = 2) neurosphere cultures. (**f**) qRT-PCR analysis of *fbw7, c-jun, bad, bim* and *bcl2* transcripts in *fbw7*$^{f/f}$, *fbw7*$^{\Delta N}$ and *fbw7*$^{\Delta N}$; *c-jun*$^{\Delta N/+}$ neurosphere cells. The data are normalised to *gapdh* and represented as fold change over RNA levels in *fbw7*$^{f/f}$ neurosphere cells, which is set to 1. Error bars represent the s.e.m. Statistical significance: n.s.: not significant; *: $p \leq 0.05$; **: $p \leq 0.01$; ***: $p \leq 0.001$ (unpaired *t* test).

**Figure 6** Fbw7 controls stem cell differentiation by antagonising Notch. (**a**) Immunohistochemistry for activated Notch1 (NICD1; red) on representative sections of the *fbw7*$^{f/f}$, *fbw7*$^{\Delta N}$ and *fbw7*$^{\Delta N}$; *Notch1*$^{\Delta/+}$ E18.5 cortex. DNA (blue) was counterstained with DAPI. Scale bars: 50 μm. DAB staining for (**b**) Nestin and (**c**) BLBP on the *fbw7*$^{f/f}$, *fbw7*$^{\Delta N}$ and *fbw7*$^{\Delta N}$; *Notch1*$^{\Delta/+}$ E18.5 cortex. Cells are counterstained with H&E. Scale bars: 50 μm. (**d**) Quantification of BLBP-positive cells in the IZ and the CP of the *fbw7*$^{f/f}$, *fbw7*$^{\Delta N}$ and *fbw7*$^{\Delta N}$; *Notch1*$^{\Delta/+}$ E18.5 cortex. n = 3. (**e**) qRT-PCR analysis of *hes5, hey1* and *hes1* transcripts in *fbw7*$^{f/f}$, *fbw7*$^{f/f}$; *Notch1*$^{\Delta/+}$, *fbw7*$^{\Delta N}$ and *fbw7*$^{\Delta N}$; *Notch1*$^{\Delta/+}$ neurospheres. The data are normalised to *gapdh* and represented as fold change over RNA levels in *fbw7*$^{f/f}$ neurospheres, which is set to 1. (**f**) Immunocytochemistry for Nestin (green) on *fbw7*$^{f/f}$, *fbw7*$^{f/f}$; *Notch1*$^{\Delta/+}$, *fbw7*$^{\Delta N}$ and *fbw7*$^{\Delta N}$; *Notch1*$^{\Delta/+}$ neurosphere cultures after 5 days under

differentiation conditions. White squares mark areas shown in high magnification in panels on the right. DNA (blue) was counterstained with Hoechst 33342. Scale bars: 50 μm. (**g**) Histogram showing the percentage of Nestin-positive cells in *fbw7*$^{f/f}$, *fbw7*$^{f/f}$; *Notch1*$^{\Delta/+}$, *fbw7*$^{\Delta N}$ and *fbw7*$^{\Delta N}$; *Notch1*$^{\Delta/+}$ neurosphere cultures after 5 days under differentiation conditions. n = 3.

Error bars represent the s.e.m. Statistical significance: n.s.: not significant; *: $p \leq 0.05$; **: $p \leq 0.01$; ***: $p \leq 0.001$ (unpaired *t* test). CP: cortical plate, IZ: intermediate zone, SVZ: subventricular zone, VZ: ventricular zone.

## SUPPLEMENTARY FIGURE LEGENDS

**Supplementary Figure 1** Efficient *fbw7* deletion in *fbw7*$^{\Delta N}$ mice. (**a**) Schematic representation of the targeting construct before and after Cre recombination. Exon 5 of the *fbw7* allele is flanked by loxP-sites (*fbw7*$^{f}$) and excised upon crossing *fbw7*$^{f/f}$ mice to transgenic mice expressing Cre recombinase. Conditional knockout of *fbw7* in the brain occurs by expressing Cre under the control of a Nestin promoter (*fbw7*$^{\Delta N}$). (**b**) *fbw7* (exon 2–5 specific probe) *in situ* hybridisation with Giemsa counterstain (blue). Rectangles mark comparable regions of the cortex (1, 1') and the eye (2, 2') shown below in high magnification for *fbw7*$^{f/f}$ and *fbw7*$^{\Delta N}$ E18.5 heads. Scale bars: 100 μm.

**Supplementary Figure 2** Cortex size in the *fbw7*$^{\Delta N}$ brain. (**a**) Schematic representation of the E18.5 mouse forebrain (fb; green) and midbrain (mb; red) dorsal view. Comparable sagittal sections of *fbw7*$^{f/f}$ and *fbw7*$^{\Delta N}$ E18.5 heads were taken alongside the lateral-medial axis (1, 2, 3) and are shown in (**b**) stained with H&E. Scale bars: in 1, 580 μm; in 2, 730 μm; in 3, 870

μm.

**Supplementary Figure 3** Decreased cellularity in the *fbw7*$^{\Delta N}$ brain. Haematoxylin and eosin (H&E) staining of the E18.5 (**a**) cerebellum and (**b**) thalamus from *fbw7*$^{f/f}$ and *fbw7*$^{\Delta N}$ mouse embryos. Rectangles mark comparable regions shown below in high magnification. Scale bars: 50 μm.

**Supplementary Figure 4** Loss of Fbw7 does not affect proliferation *in vivo*. DAB staining for the S-phase marker Ki67 on representative sections of the *fbw7*$^{f/f}$ and *fbw7*$^{\Delta N}$ cortex at (**a**) E10.5, (**b**) E14.5, (**c**) E16.5 and (**d**) E18.5. Cells are counterstained with H&E. Scale bars: 50 μm. (**e**) Quantification of Ki67-positive cells in the E10.5 *fbw7*$^{f/f}$ and *fbw7*$^{\Delta N}$ cortex and in the SVZ of the E14.5, E16.5 and E18.5 *fbw7*$^{f/f}$ and *fbw7*$^{\Delta N}$ cortex. n = 3.
Error bars represent the s.e.m. CP: cortical plate, IZ: intermediate zone, SVZ: subventricular zone, VZ: ventricular zone.

**Supplementary Figure 5** Reduced number of neuroblasts in the *fbw7*$^{\Delta N}$ cortex. DAB staining for Doublecortin (Dcx) in the (**a**) E18.5, (**b**) E16.5 and (**c**) E14.5 *fbw7*$^{f/f}$ and *fbw7*$^{\Delta N}$ cortex. Black rectangles mark areas shown in high magnification in panels at the top. Cells are counterstained with H&E. Scale bars: 50 μm. (**d**) Quantification of Dcx-positive cells in the SVZ of the E18.5 (n = 4), E16.5 (n = 3) and E14.5 (n = 3) *fbw7*$^{f/f}$ and *fbw7*$^{\Delta N}$ cortex.
Error bars represent the s.e.m. Statistical significance: *: $p \leq 0.05$; **: $p \leq 0.01$ (unpaired *t* test). CP: cortical plate, IZ: intermediate zone, SVZ: subventricular zone, VZ: ventricular zone.

**Supplementary Figure 6** Loss of Fbw7 does not affect gliogenesis. (**a**)

Immunohistochemistry for GFAP (red) on representative sections of the *fbw7*$^{f/f}$ and *fbw7*$^{\Delta N}$ E18.5 cortex. DNA (blue) was counterstained with DAPI. Scale bars: 50 μm. DAB staining for (**b**) S100 and (**d**) NG2 in the CP of the E18.5 *fbw7*$^{f/f}$ and *fbw7*$^{\Delta N}$ cortex. Red arrowheads denote positive cells. Scale bars: 50 μm. Quantification of (**c**) S100-positive and (**e**) NG2-positive cells in the IZ and the CP of the E18.5 *fbw7*$^{f/f}$ and *fbw7*$^{\Delta N}$ cortex. n = 3. DAB staining for (**f**) S100 and (**h**) NG2 on *fbw7*$^{f/f}$ and *fbw7*$^{\Delta N}$ neurosphere sections. Red arrowheads denote positive cells. Scale bars: 50 μm. Quantification of (**g**) S100-positive and (**i**) NG2-positive cells in *fbw7*$^{f/f}$ and *fbw7*$^{\Delta N}$ neurospheres. n = 3.

Error bars represent the s.e.m. Statistical significance: n.s.: not significant (unpaired *t* test). CP: cortical plate, IZ: intermediate zone, SVZ: subventricular zone, VZ: ventricular zone.

**Supplementary Figure 7** Increased stem cell and decreased neuronal marker expression in the *fbw7*$^{\Delta N}$ tectum. From left to right: Immunohistochemistry for Musashi1 (Msi1; red), BLBP (red), Nestin (red) and NeuN (green) on representative sections of the *fbw7*$^{f/f}$ and *fbw7*$^{\Delta N}$ E18.5 tectum. DNA (blue) was counterstained with DAPI. ML: mantle layer, VZ: ventricular zone. Scale bars: 50 μm.

**Supplementary Figure 8** Loss of Fbw7 does not affect proliferation *in vitro*. (**a**) Immunocytochemistry for serine 10 phosphorylated histone H3 (pH3; red) on *fbw7*$^{f/f}$ and *fbw7*$^{\Delta N}$ neurosphere sections. DNA (blue) was counterstained with DAPI. Arrowheads denote pH3-positive cells. Scale bars: 50 μm. (**b**) FACS histograms showing carboxyfluorescein diacetate succinimidyl ester (CFSE) intensity in *fbw7*$^{f/f}$ and *fbw7*$^{\Delta N}$ neurosphere cultures 1 (d1), 3 (d3), 5 (d5) and 7 (d7) days after CFSE staining. u: unstained control. (**c**) Histogram showing the loss of CFSE intensity (in %) over time (in days). (**d**) Histogram showing cell division rates of *fbw7*$^{f/f}$ and *fbw7*$^{\Delta N}$ neurosphere cells based on the loss of CFSE intensity.

Error bars represent the s.e.m.

**Supplementary Figure 9** *fbw7*$^{\Delta N}$ neurospheres exhibit differentiation defect. (**a**) Phase contrast pictures of *fbw7*$^{f/f}$ and *fbw7*$^{\Delta N}$ neurosphere cultures under differentiation conditions. (**b**) Stainings for DNA (blue) with Hoechst 33342 on *fbw7*$^{f/f}$ and *fbw7*$^{\Delta N}$ neurosphere cultures after 5 days of differentiation. Scale bars: 50 μm.

**Supplementary Figure 10** Increased stem cell marker expression in *fbw7*$^{\Delta N}$ neurosphere differentiation cultures. Immunocytochemistry for (**a**) Vimentin (green) and BLBP (red) and (**b**) CD133 (green) on *fbw7*$^{f/f}$ and *fbw7*$^{\Delta N}$ neurosphere cultures after 5 days under differentiation conditions. White squares mark areas shown in high magnification in panels on the right. DNA (blue) was counterstained with Hoechst 33342. Scale bars: 100 μm.

**Supplementary Figure 11** Loss of Fbw7 leads to similar results in adherent NSC cultures in comparison to neurosphere cultures. (**a**) Phase contrast pictures of *fbw7*$^{f/f}$ and *fbw7*$^{\Delta N}$ adherent NSC cultures under self-renewal conditions. Scale bars: 50 μm. Immunocytochemistry for Nestin (green) on *fbw7*$^{f/f}$ and *fbw7*$^{\Delta N}$ adherent NSC cultures (**b**) under self-renewal conditions and (**c**) after 5 days under differentiation conditions. Scale bars: 50 μm. (**d**) Quantification of Nestin-positive cells in *fbw7*$^{f/f}$ and *fbw7*$^{\Delta N}$ adherent NSC cultures after 5 days under differentiation conditions. (**e**) Western blot analysis of Fbw7, serine 73 phosphorylated c-Jun (p-c-Jun), activated Notch1 (NICD1), threonine 58/serine 62 phosphorylated c-Myc (p-c-Myc), threonine 395 phosphorylated cyclinE and β-Actin on protein lysates from *fbw7*$^{f/f}$ and *fbw7*$^{\Delta N}$ adherent NSC cultures (cropped images, full-length blots are presented in **Supplementary Fig. 15b**). (**f**) qRT-PCR analysis of *fbw7, c-jun* and *hes5* transcripts in cells

from *fbw7*$^{f/f}$ and *fbw7*$^{\Delta N}$ adherent NSC cultures. The data are normalised to *gapdh* and represented as fold change over RNA levels in *fbw7*$^{f/f}$ adherent NSCs, which is set to 1.
Error bars represent the s.e.m. Statistical significance: *: $p \leq 0.05$ (unpaired *t* test).

**Supplementary Figure 12** Increased number of immature cells in *fbw7*$^{\Delta N}$ neurosphere cultures after prolonged time under differentiation conditions. Immunocytochemistry for Nestin (green) on *fbw7*$^{f/f}$ and *fbw7*$^{\Delta N}$ neurosphere cultures after 11 days of differentiation. White squares mark areas shown in high magnification in panels on the right. DNA (blue) was counterstained with Hoechst 33342. Scale bars: 100 μm.

**Supplementary Figure 13** Loss of Fbw7 does not affect neurosphere multipotentiality. Immunocytochemistry for Map2 (green), O4 (red) and Connexin43 (Cx43; magenta) on *fbw7*$^{f/f}$ and *fbw7*$^{\Delta N}$ neurosphere cultures after 5 days of differentiation. DNA (blue) was counterstained with Hoechst 33342. Scale bars: 50 μm.

**Supplementary Figure 14** *fbw7* isoform expression. qRT-PCR analysis showing the relative abundance of *fbw7* isoforms α, β and γ in *fbw7*$^{f/f}$ neurospheres, adult brain, skeletal muscle and liver normalised to *gapdh* expression. Expression of *fbw* α is set to 1. Error bars represent the standard deviation (s.d.).

**Supplementary Figure 15** Full-length Western Blots. Full-length Western Blots from (**a**) **Fig. 5a** and (**b**) **Supplementary Fig. 11e**. Molecular weight standards are shown in kDa.

**Supplementary Figure 16** Decreased cellularity in *fbw7*$^{\Delta N}$ brains is c-Jun-dependent.

Haematoxylin and eosin (H&E) staining of comparable regions of the *fbw7*$^{f/f}$, *fbw7*$^{\Delta N}$ and *fbw7*$^{\Delta N}$; *c-jun*$^{\Delta N/+}$ E18.5 midbrain. Rectangles mark the area of the tectum shown below in high magnification. ML: mantle layer, VZ: ventricular zone. Scale bars: 200 µm.

**Supplementary Figure 17** Differentiation defect in *fbw7*$^{\Delta N}$ neurosphere cultures is not c-Jun-dependent. Histogram showing the percentage of Nestin-positive cells in *fbw7*$^{f/f}$ (n = 8), *fbw7*$^{\Delta N}$ (n = 11) and *fbw7*$^{\Delta N}$*c-jun*$^{\Delta N/+}$ (n = 2) neurosphere cultures after 5 days of differentiation. Error bars represent the s.e.m. Statistical significance: n.s.: not significant; ***: $p \leq 0.001$ (unpaired *t* test).

**Supplementary Figure 18** Notch downregulation rescues neuronal numbers. (**a**) DAB staining for NeuN on the E18.5 *fbw7*$^{f/f}$, *fbw7*$^{\Delta N}$ and *fbw7*$^{\Delta N}$; *Notch1*$^{\Delta/+}$ cortex. Cells are counterstained with H&E. Scale bars: 50 µm. (**b**) Quantification of NeuN-positive cells in the IZ and the CP of the E18.5 *fbw7*$^{f/f}$, *fbw7*$^{\Delta N}$ and *fbw7*$^{\Delta N}$; *Notch1*$^{\Delta/+}$ cortex (n = 3). (**c**) Immunocytochemistry for Map2 (green) on *fbw7*$^{f/f}$, *fbw7*$^{\Delta N}$ and *fbw7*$^{\Delta N}$; *Notch1*$^{\Delta/+}$ neurosphere cultures after 5 days under differentiation conditions. White squares mark areas shown in high magnification in panels on the right. DNA (blue) was counterstained with Hoechst 33342. Scale bars: 50 µm. (**d**) Histogram showing the percentage of Map2-positive cells in *fbw7*$^{f/f}$ (n = 3), *fbw7*$^{\Delta N}$ (n = 4) and *fbw7*$^{\Delta N}$; *Notch1*$^{\Delta/+}$ (n = 5) neurosphere cultures after 5 days under differentiation conditions.

Error bars represent the s.e.m. Statistical significance: *: $p \leq 0.05$; **: $p \leq 0.01$ (unpaired *t* test). CP: cortical plate, IZ: intermediate zone, SVZ: subventricular zone, VZ: ventricular zone.

**Supplementary Figure 19** Inhibition of Notch signalling alleviates the block in stem cell

differentiation. (**a**) qRT-PCR analysis of *hes5*, *hey1* and *hes1* transcripts in *fbw7*$^{f/f}$ and *fbw7*$^{\Delta N}$ neurospheres treated with DMSO (control) or 1 μM DAPT. The data are normalised to *gapdh* and represented as fold change over RNA levels in *fbw7*$^{f/f}$ + DMSO neurospheres, which is set to 1. (**b**) Immunocytochemistry for Nestin (green) on *fbw7*$^{f/f}$ and *fbw7*$^{\Delta N}$ neurosphere cultures after 5 days under differentiation conditions treated with DMSO (control) or 1 μM DAPT. White squares mark areas shown in high magnification in panels on the right. DNA (blue) was counterstained with Hoechst 33342. Scale bars: 100 μm. (**c**) Histogram showing the percentage of Nestin-positive cells in *fbw7*$^{f/f}$ and *fbw7*$^{\Delta N}$ neurosphere cultures after 5 days under differentiation conditions treated with DMSO (control) or 1 μM DAPT. n = 5. Error bars represent the s.e.m. Statistical significance: n.s.: not significant; **: $p \leq 0.01$; ***: $p \leq 0.001$ (unpaired *t* test).

**ACKNOWLEDGEMENTS**

We are grateful to the Animal Unit, Equipment Park, FACS Lab and the Experimental Pathology Lab at the London Research Institute for technical help and advice on histology. We are grateful to F. Radke for floxed Notch1 mice. We thank R. Sancho for the data on *fbw7* isoform expression in various tissues. We thank C. R. Da Costa, S. Marino and A. Martin-Villalba for critical reading of the manuscript. S.M.B. is supported by a Federation of the Societies of Biochemistry and Molecular Biology (FEBS) Long Term Fellowship. Part of this work is supported by an MRC project grant (85704) to A.B. The London Research Institute is funded by Cancer Research UK.

**AUTHOR CONTRIBUTIONS**

J.D.H. designed and conducted the majority of the experiments, did the data analyses and co-wrote the manuscript. A.J. generated the *fbw7*$^{f/f}$ mice and performed the radioactive ISH. S.M.B. performed the experiments on adherent NSC cultures. E.N. did the IHC stainings. B.S.-D. performed the non-radioactive ISH. S.B. gave advice on neurosphere sectioning. A.B. supervised the project, directed the experiments and wrote the manuscript.

## MATERIALS AND METHODS

### Mouse Lines

The *fbw7* (floxed exon 5) transgenic construct was electroporated into embryonic stem cells, stable transfectants were selected and mice generated according to standard protocols[7]. Details will be described in Jandke et al., *in preparation*. *c-jun*$^{f/f}$, *Notch1*$^{f/f}$ and Nestin-Cre mice have been described[9,26]. All experiments involving mice were approved by the London Research Institute (LRI) Animal Ethics Committee following Home Office guidelines.

### Cell culture

Neural cells were isolated from E14.5 fore- and midbrains of *fbw7*$^{f/f}$, *fbw7*$^{f/f}$; *Notch1*$^{\Delta/+}$, *fbw7*$^{\Delta N}$, *fbw7*$^{\Delta N}$; *c-Jun*$^{\Delta N/+}$ and *fbw7*$^{\Delta N}$; *Notch1*$^{\Delta/+}$ mouse embryos. Cells were cultured under self-renewal conditions in Neurobasal Medium (Invitrogen) supplemented with 1% Penicillin/Streptomycin (10000 U/ml; Invitrogen), 1% L-glutamine (200 mM; Invitrogen), 2% B27 supplement (Invitrogen) and human epidermal growth factor (EGF; 20 ng/ml; PeproTech) and fibroblast growth factor (FGF-basic; 20 ng/ml; PeproTech). All experiments were performed using secondary and tertiary neurospheres.

Adherent NSC cultures were derived as previously described[43] with minor modifications. Briefly, cells were cultured in Neurobasal Medium (Invitrogen) supplemented with 1% Penicillin/Streptomycin (10000 U/ml; Invitrogen), 1% L-glutamine (200 mM; Invitrogen), 2% B27 supplement (Invitrogen), 1% N-2 supplement (Invitrogen), 20 ng/ml EGF (PeproTech), 20 ng/ml FGF-basic (PeproTech) and 1 µg/ml laminin (Sigma).

For differentiation, growth factors were withdrawn from the medium and 10% NeuroCult® Differentiation Supplement (StemCell Technologies) was added. Under differentiation conditions, 5 x $10^5$ cells were plated on poly-L-ornithine (0.01% solution; Sigma; diluted 1:10 in 150 mM disodium tetraborate; Sigma) coated cover slips.

Single cell suspensions were made from neurospheres using AccuMax (PAA Laboratories).

To assess neurosphere formation, cells were plated in limiting dilutions from 500 to 4 cells in 96-well-plates. Neurospheres were counted after 2 weeks in culture.

To examine cell division rates, neurosphere-derived cells were stained with carboxyfluorescein diacetate succinimidyl ester (CFSE) using the CellTrace™ CFSE Cell Proliferation Kit (Invitrogen) according to the manufacturer's instructions. FACS-measurements for CFSE intensity were performed every 48 h after CFSE-staining for one week using an LSR II Flow Cytometer (BD). By means of DAPI-staining, viable cells (DAPI-negative) were selected. Analysis was carried out using CellQuest™ Pro (BD) and FlowJo (Tree Star) software.

For the inhibition of Notch signalling, neurospheres were treated with 1 µM N-[N-(3,5-Difluorophenacetyl-L-Alanyl)]-S-phenylglycine t-butyl ester (DAPT; Sigma) for 72 h.

**Immunohistochemistry and immunocytochemistry**

Mouse brains were dissected from E10.5, E14.5, E16.5 and E18.5 *fbw7*$^{f/f}$, *fbw7*$^{\Delta N}$, *fbw7*$^{\Delta N}$; *c-Jun*$^{\Delta N/+}$ and *fbw7*$^{\Delta N}$; *Notch1*$^{\Delta/+}$ mouse embryos. Brains were fixed in 10% neutral buffered formalin overnight, transferred to 70% ethanol, processed and embedded into paraffin. Neurospheres were fixed in 10% neutral buffered formalin overnight and processed using the Shandon Cytoblock® Cell Preparation System (Thermo Fisher Scientific). Sections were cut (for brain sections: sagittally) at 4 µm for Haematoxylin & Eosin (H&E) staining, 3,3'-Diaminobenzidine (DAB) staining, TUNEL (TdT-mediated dUTP-biotin nick end labeling) and fluorescent immunohistochemistry. To define comparable sections, brains were cut alongside the medial-lateral axis with every 10$^{th}$ section stained with H&E. For cell counting, all cells in the tectal ML and VZ as well as in the CP, IZ, SVZ and VZ of the cortex were counted in an area of the same width. Layer boundaries were determined by cell morphology and layer-specific marker expression.

Cells from neurosphere differentiation cultures were fixed in ice-cold methanol for 3 mins or in 4% paraformaldehyde for 20 mins. For immunohistochemistry and immunocytochemistry, antibodies against activated Notch1 (Abcam), active Caspase3 (R&D), BLBP (Abcam), Brn2 (Santa Cruz Biotechnology), CD133 (Prominin 1; eBioscience), Connexin43 (Zymed), Ctip2 (Abcam), serine 73 phosphorylated c-Jun (Cell Signaling), Doublecortin (Santa Cruz Biotechnology), GLAST (LifeSpan Biosciences), serine 10 phosphorylated histone H3 (pH3; Millipore), Ki67 (DAKO), Map2 (Sigma), Musashi1 (Chemicon), Nestin (IHC: Chemicon; ICC: BD (monoclonal); Abcam (polyclonal)), NeuN (Chemicon), NG2 (Chemicon), O4 (Chemicon), RC2 (DSHB), S100 (Abcam), Tbr1 (Abcam), Tbr2 (Abcam) and Vimentin (Abcam) were used. DNA was counterstained with 4'-6-Diamidino-2-phenylindole (DAPI; Sigma) or Hoechst 33342 (Sigma).

### *In situ* hybridisation

Radioactive *in situ* hybridisation (ISH) was performed by the CRUK *in situ* hybridisation service at the LRI. The *in situ* probe corresponded to exon 2–5 of the murine *fbw7* cDNA.

Non-radioactive ISH was performed as previously described[44] with minor modifications. For *fbw7* ISH, DIG-labelled 800 bp PCR product (exons 6 to 10) was used.

### Western Blot Analysis

Neurospheres were suspended in cell lysis buffer (Cell Signaling) supplemented with protease inhibitor cocktail (Sigma). Western blot analysis was performed as previously described[45]. For immunoblotting, antibodies against activated Notch1 (Abcam), c-Jun (Santa Cruz Biotechnology), serine 73 phosphorylated c-Jun (Cell Signaling), Fbw7 (LRI/CRUK; Abcam), threonine 58/serine 62 phosphorylated c-Myc (Cell Signaling), threonine 395 phosphorylated cyclinE (Santa Cruz Biotechnology) and β-Actin (Sigma) were used.

**qRT-PCR analysis**

For qRT-PCR analysis, total mRNA was isolated from neurospheres using the RNeasy Mini-kit (QIAGEN) according to the manufacturer's instructions. cDNA was synthesized using Invitrogen Superscript III reagents according to the manufacturer's instructions. Quantitative real-time PCR was performed measuring SYBR Green incorporation (Platinum® Quantitative PCR SuperMix-UDG w/ROX, Invitrogen) on an ABI7900HT (Applied Bioscience). Data were analyzed using the SDS 2.3 software. The following primers were used for murine cell qRT-PCR analysis:

F-Bad: 5'-CAGGGAGAAGAGCTGACGTACA-3'

R-Bad: 5'-CCACCCCTCCGTGGCTAT-3'

F-Bcl2 (beta): 5'-GCTCCCCTGACCTCTCACTCT-3'

R-Bcl2 (beta): 5'-CTGGATTCTTGCTCCCTCACA-3'

F-Bim: 5'-CCCCTACCTCCCTACAGACAGA-3'

R-Bim: 5'-GCGCAGATCTTCAGGTTCCT-3'

F-c-Jun: 5'-TGAAAGCTGTGTCCCCTGTC-3'

R-c-Jun: 5'-ATCACAGCACATGCCACTTC-3'

F-Fbw7α: 5'-CTGACCAGCTCTCCTCTCCATT-3'

R-Fbw7α: 5'-GCTGAACATGGTACAAGGCCA-3'

F-Fbw7β: 5'-TTGTCAGAGACTGCCAAGCAG-3'

R-Fbw7β: 5'-GACTTTGCATGGTTTCTTTCCC-3'

F-Fbw7γ: 5'-AACCATGGCTTGGTTCCTGTTG-3'

R-Fbw7γ: 5'-CAGAACCATGGTCCAACTTTC-3'

F-Fbw7 (exon5): 5'-TTCATTCCTGGAACCCAAAGA-3'

R-Fbw7 (exon5): 5'-TCCTCAGCCAAAATTCTCCAGTA-3'

F- Gapdh: 5’- TGAAGCAGGCATCTGAGGG -3’

R-Gapdh: 5’-CGAAGGTGGAAGAGTGGGAG -3’

F-Hes1: 5’-TCAGCGAGTGCATGAACGA-3’

R-Hes1: 5’-TGCGCACCTCGGTGTTAAC-3’

F-Hes5: 5’-TGCAGGAGGCGGTACAGTTC-3’

R-Hes5: 5’-GCTGGAAGTGGTAAAGCAGCTT-3’

F-Hey1: 5’-GGCAGCCCTAAGCACTCTCA-3’

R-Hey1: 5’-TTCAGACTCCGATCGCTTACG-3’

**Statistical Analysis**

Statistical evaluation was performed by Student’s unpaired *t* test. Data are presented as mean ± standard error of the mean (s.e.m.). *: $p \leq 0.05$ was considered statistically significant, **: $p \leq 0.01$ was considered very statistically significant, ***: $p \leq 0.001$ was considered extremely statistically significant.

## REFERENCES


1. Merkle, F.T. & Alvarez-Buylla, A. Neural stem cells in mammalian development. *Curr Opin Cell Biol* **18**, 704–709 (2006).
2. Gotz, M. & Barde, Y.A. Radial glial cells defined and major intermediates between embryonic stem cells and CNS neurons. *Neuron* **46**, 369–372 (2005).
3. Ho, M.S., Tsai, P.I. & Chien, C.T. F-box proteins: the key to protein degradation. *J Biomed Sci* **13**, 181–191 (2006).
4. Welcker, M. & Clurman, B.E. FBW7 ubiquitin ligase: a tumour suppressor at the crossroads of cell division, growth and differentiation. *Nat Rev Cancer* **8**, 83–93 (2008).
5. Tan, Y., Sangfelt, O. & Spruck, C. The Fbxw7/hCdc4 tumor suppressor in human cancer. *Cancer Lett* **271**, 1–12 (2008).
6. Fuchs, S.Y. Tumor suppressor activities of the Fbw7 E3 ubiquitin ligase receptor. *Cancer Biol Ther* **4**, 506–508 (2005).
7. Behrens, A., Sibilia, M. & Wagner, E.F. Amino-terminal phosphorylation of c-Jun regulates stress-induced apoptosis and cellular proliferation. *Nat Genet* **21**, 326–329 (1999).
8. Besirli, C.G., Wagner, E.F. & Johnson, E.M., Jr. The limited role of NH2-terminal c-Jun phosphorylation in neuronal apoptosis: identification of the nuclear pore complex as a potential target of the JNK pathway. *J Cell Biol* **170**, 401–411 (2005).
9. Raivich, G., *et al.* The AP-1 transcription factor c-Jun is required for efficient axonal regeneration. *Neuron* **43**, 57–67 (2004).
10. Yoon, K.J., *et al.* Mind bomb 1-expressing intermediate progenitors generate notch signaling to maintain radial glial cells. *Neuron* **58**, 519–531 (2008).
11. Mizutani, K., Yoon, K., Dang, L., Tokunaga, A. & Gaiano, N. Differential Notch signalling distinguishes neural stem cells from intermediate progenitors. *Nature* **449**, 351–355 (2007).
12. Corbin, J.G., *et al.* Regulation of neural progenitor cell development in the nervous system. *J Neurochem* **106**, 2272–2287 (2008).
13. Yoon, K. & Gaiano, N. Notch signaling in the mammalian central nervous system: insights from mouse mutants. *Nat Neurosci* **8**, 709–715 (2005).
14. Tetzlaff, M.T., *et al.* Defective cardiovascular development and elevated cyclin E and Notch proteins in mice lacking the Fbw7 F-box protein. *Proc Natl Acad Sci U S A* **101**, 3338–3345 (2004).
15. Tsunematsu, R., *et al.* Mouse Fbw7/Sel-10/Cdc4 is required for notch degradation during vascular development. *J Biol Chem* **279**, 9417–9423 (2004).
16. Kramer, E.R., *et al.* Cooperation between GDNF/Ret and ephrinA/EphA4 signals for motor-axon pathway selection in the limb. *Neuron* **50**, 35–47 (2006).
17. Hartfuss, E., Galli, R., Heins, N. & Gotz, M. Characterization of CNS precursor subtypes and radial glia. *Dev Biol* **229**, 15–30 (2001).
18. Reynolds, B.A. & Rietze, R.L. Neural stem cells and neurospheres--re-evaluating the relationship. *Nat Methods* **2**, 333–336 (2005).
19. Nateri, A.S., Riera-Sans, L., Da Costa, C. & Behrens, A. The ubiquitin ligase SCFFbw7 antagonizes apoptotic JNK signaling. *Science* **303**, 1374–1378 (2004).
20. Bossy-Wetzel, E., Bakiri, L. & Yaniv, M. Induction of apoptosis by the transcription factor c-Jun. *EMBO J* **16**, 1695–1709 (1997).
21. Whitfield, J., Neame, S.J., Paquet, L., Bernard, O. & Ham, J. Dominant-negative c-Jun promotes neuronal survival by reducing BIM expression and inhibiting mitochondrial cytochrome c release. *Neuron* **29**, 629–643 (2001).
22. Ma, C., *et al.* dp5/HRK is a c-Jun target gene and required for apoptosis induced by potassium deprivation in cerebellar granule neurons. *J Biol Chem* **282**, 30901–30909 (2007).
23. Angel, P., Hattori, K., Smeal, T. & Karin, M. The *jun* proto-oncogene is positively autoregulated by its product, Jun/AP1. *Cell* **55**, 875–885 (1988).
24. Gaiano, N., Nye, J.S. & Fishell, G. Radial glial identity is promoted by Notch1 signaling in the murine forebrain. *Neuron* **26**, 395–404 (2000).
25. Anthony, T.E., Mason, H.A., Gridley, T., Fishell, G. & Heintz, N. Brain lipid-binding protein is a direct target of Notch signaling in radial glial cells. *Genes Dev* **19**, 1028–1033 (2005).
26. Radtke, F., *et al.* Deficient T cell fate specification in mice with an induced inactivation of Notch1. *Immunity* **10**, 547–558 (1999).
27. Selkoe, D. & Kopan, R. Notch and Presenilin: regulated intramembrane proteolysis links development and degeneration. *Annu Rev Neurosci* **26**, 565–597 (2003).
28. Anthony, T.E., Klein, C., Fishell, G. & Heintz, N. Radial glia serve as neuronal progenitors in all

regions of the central nervous system. *Neuron* **41**, 881–890 (2004).
29. Patten, B.A., Peyrin, J.M., Weinmaster, G. & Corfas, G. Sequential signaling through Notch1 and erbB receptors mediates radial glia differentiation. *J Neurosci* **23**, 6132–6140 (2003).
30. Coffey, E.T., *et al.* c-Jun N-terminal protein kinase (JNK) 2/3 is specifically activated by stress, mediating c-Jun activation, in the presence of constitutive JNK1 activity in cerebellar neurons. *J Neurosci* **22**, 4335–4345 (2002).
31. Wang, X., *et al.* Targeted deletion of the mitogen-activated protein kinase kinase 4 gene in the nervous system causes severe brain developmental defects and premature death. *Mol Cell Biol* **27**, 7935–7946 (2007).
32. Chang, L., Jones, Y., Ellisman, M.H., Goldstein, L.S. & Karin, M. JNK1 Is Required for Maintenance of Neuronal Microtubules and Controls Phosphorylation of Microtubule-Associated Proteins. *Dev Cell* **4**, 521–533 (2003).
33. Ohtsuka, T., *et al.* Hes1 and Hes5 as notch effectors in mammalian neuronal differentiation. *EMBO J* **18**, 2196–2207 (1999).
34. de la Pompa, J.L., *et al.* Conservation of the Notch signalling pathway in mammalian neurogenesis. *Development* **124**, 1139–1148 (1997).
35. Nelson, B.R., Hartman, B.H., Georgi, S.A., Lan, M.S. & Reh, T.A. Transient inactivation of Notch signaling synchronizes differentiation of neural progenitor cells. *Dev Biol* **304**, 479–498 (2007).
36. Hojo, M., *et al.* Glial cell fate specification modulated by the bHLH gene Hes5 in mouse retina. *Development* **127**, 2515–2522 (2000).
37. Thompson, B.J., *et al.* Control of hematopoietic stem cell quiescence by the E3 ubiquitin ligase Fbw7. *J Exp Med* **205**, 1395–1408 (2008).
38. Mao, J.H., *et al.* Fbxw7/Cdc4 is a p53-dependent, haploinsufficient tumour suppressor gene. *Nature* **432**, 775–779 (2004).
39. Welcker, M., Orian, A., Grim, J.E., Eisenman, R.N. & Clurman, B.E. A nucleolar isoform of the Fbw7 ubiquitin ligase regulates c-Myc and cell size. *Curr Biol* **14**, 1852–1857 (2004).
40. Sangfelt, O., Cepeda, D., Malyukova, A., van Drogen, F. & Reed, S.I. Both SCF(Cdc4alpha) and SCF(Cdc4gamma) are required for cyclin E turnover in cell lines that do not overexpress cyclin E. *Cell Cycle* **7**, 1075–1082 (2008).
41. van Drogen, F., *et al.* Ubiquitylation of cyclin E requires the sequential function of SCF complexes containing distinct hCdc4 isoforms. *Mol Cell* **23**, 37–48 (2006).
42. Matsuoka, S., *et al.* Fbxw7 acts as a critical fail-safe against premature loss of hematopoietic stem cells and development of T-ALL. *Genes Dev* **22**, 986–991 (2008).
43. Pollard, S.M., Conti, L., Sun, Y., Goffredo, D. & Smith, A. Adherent neural stem (NS) cells from fetal and adult forebrain. *Cereb Cortex* **16 Suppl 1**, i112–120 (2006).
44. Behrens, A., *et al.* Impaired intervertebral disc formation in the absence of Jun. *Development* **130**, 103–109 (2003).
45. Nateri, A.S., Spencer-Dene, B. & Behrens, A. Interaction of phosphorylated c-Jun with TCF4 regulates intestinal cancer development. *Nature* **437**, 281–285 (2005).

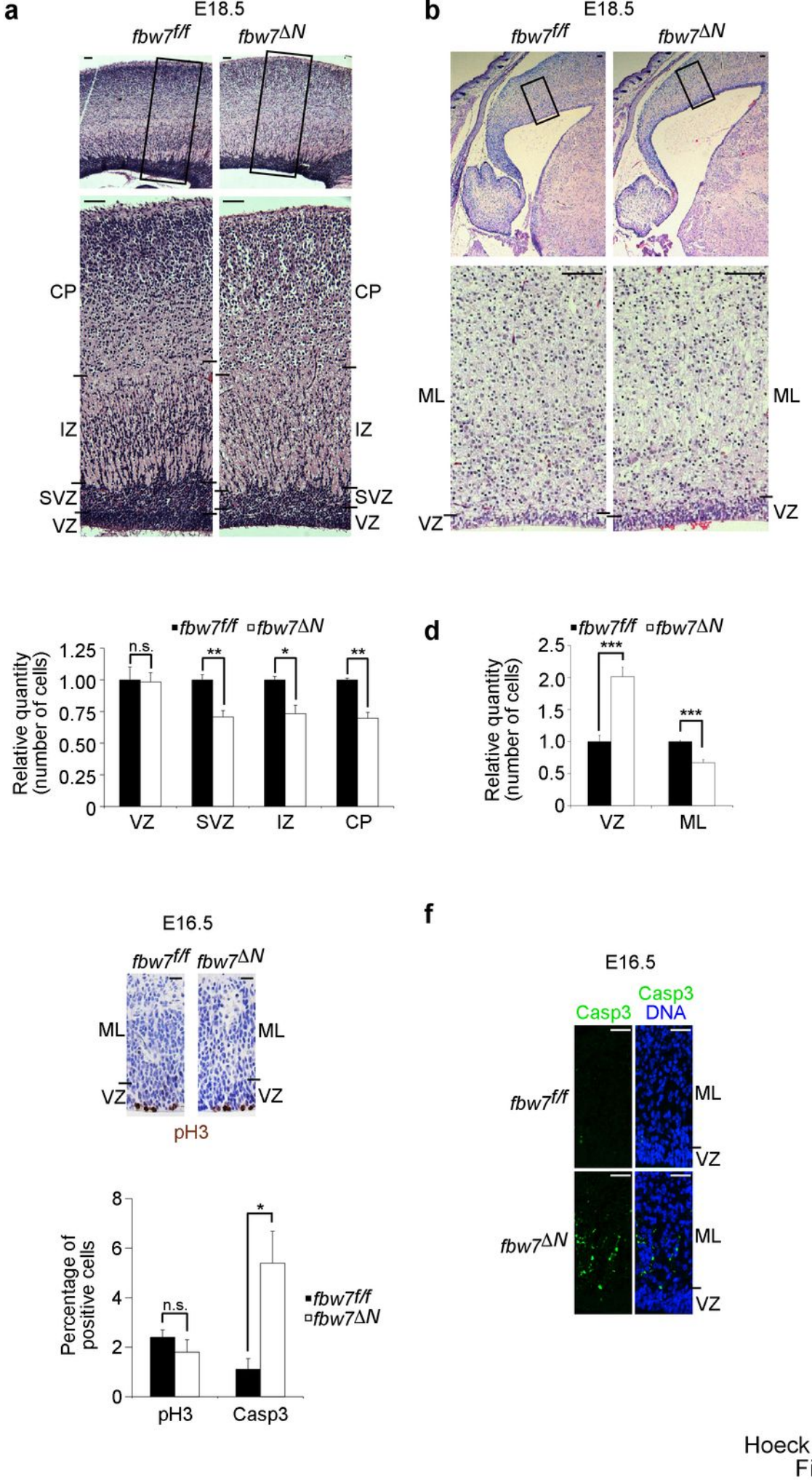


Hoeck *et al.*, 2010
Figure 1

Hoeck *et al.*, 2010
Figure 2

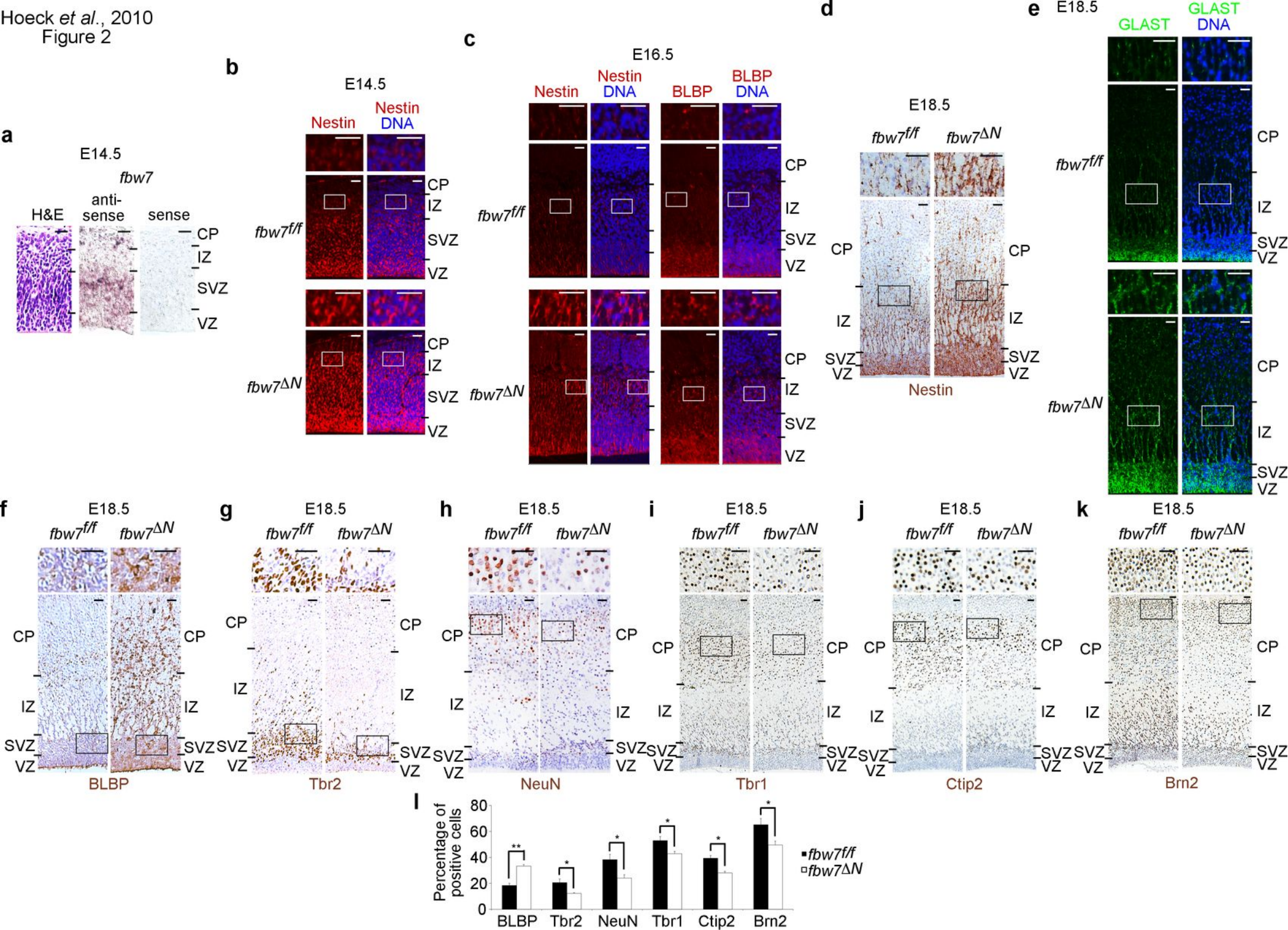

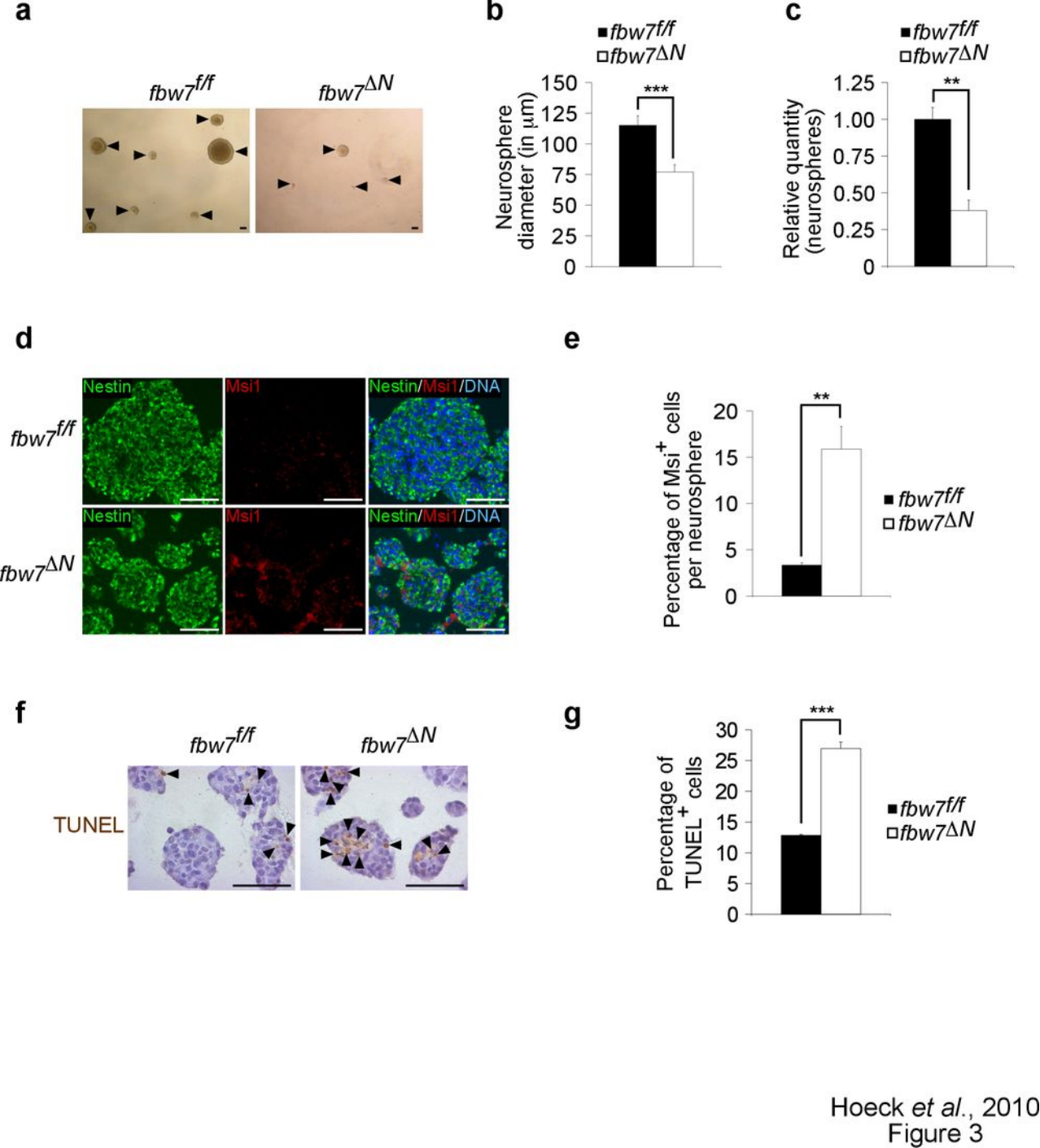


Hoeck *et al.*, 2010
Figure 3

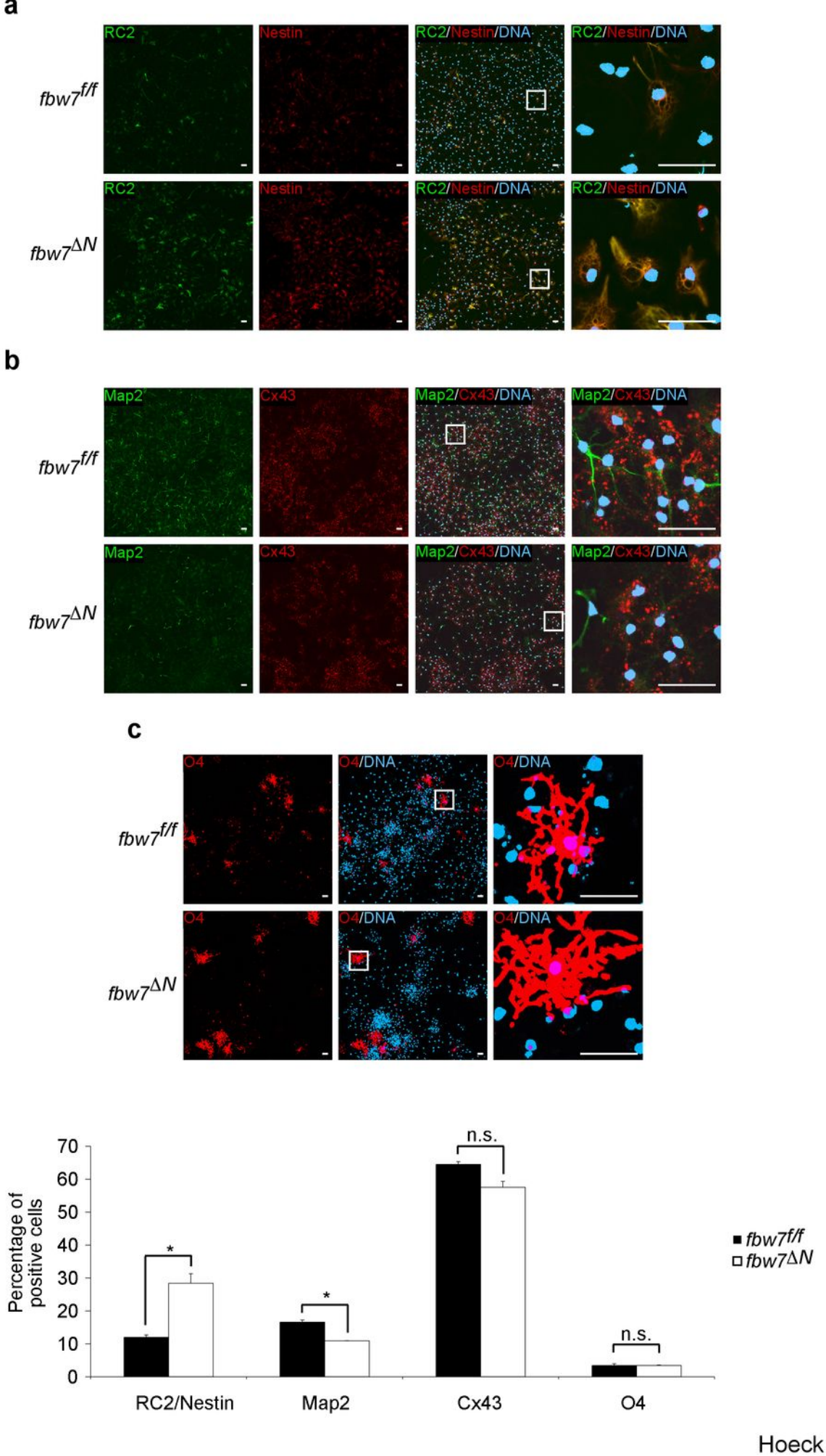


Hoeck *et al.*, 2010
Figure 4

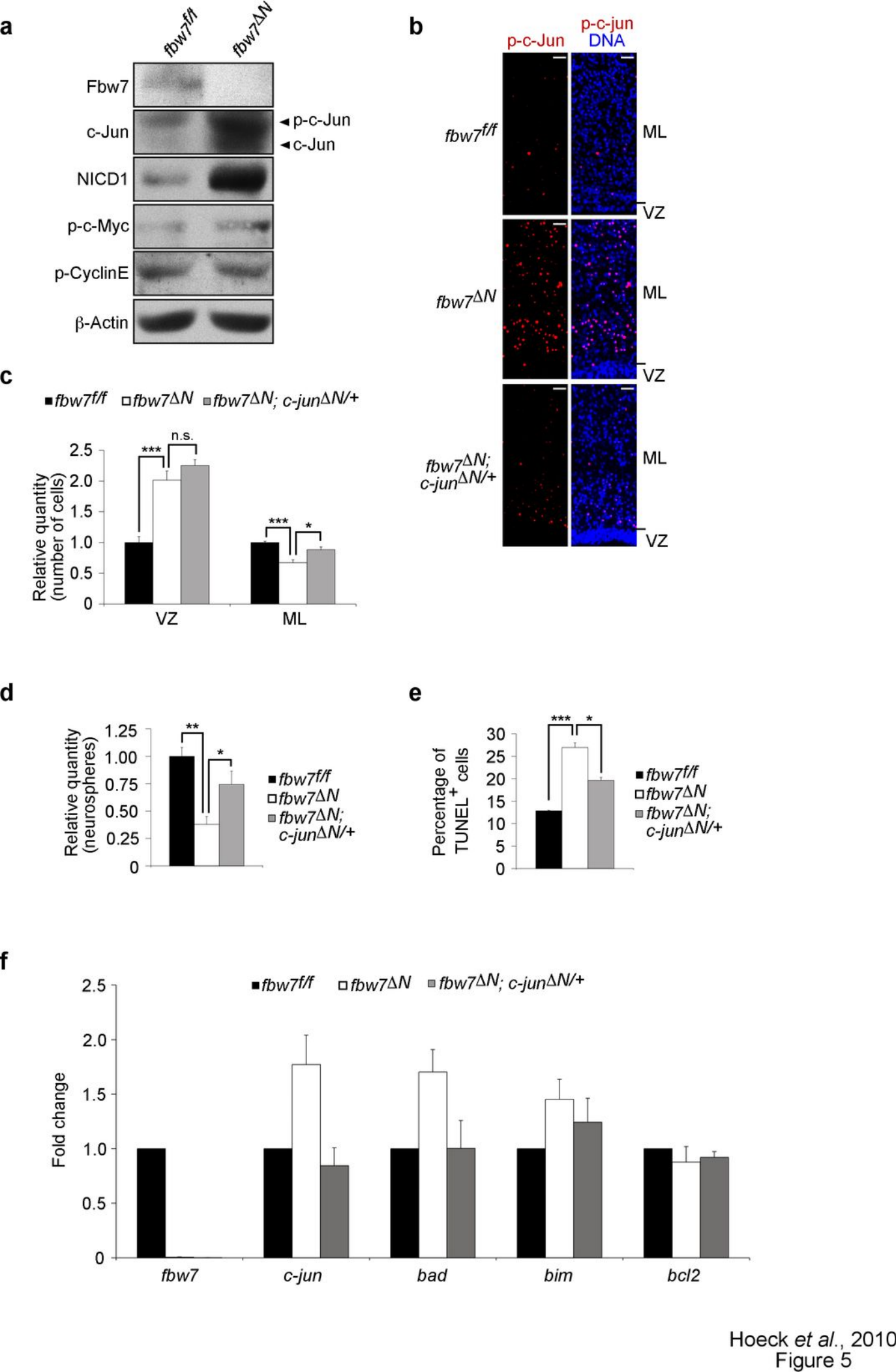


Hoeck *et al.*, 2010
Figure 5

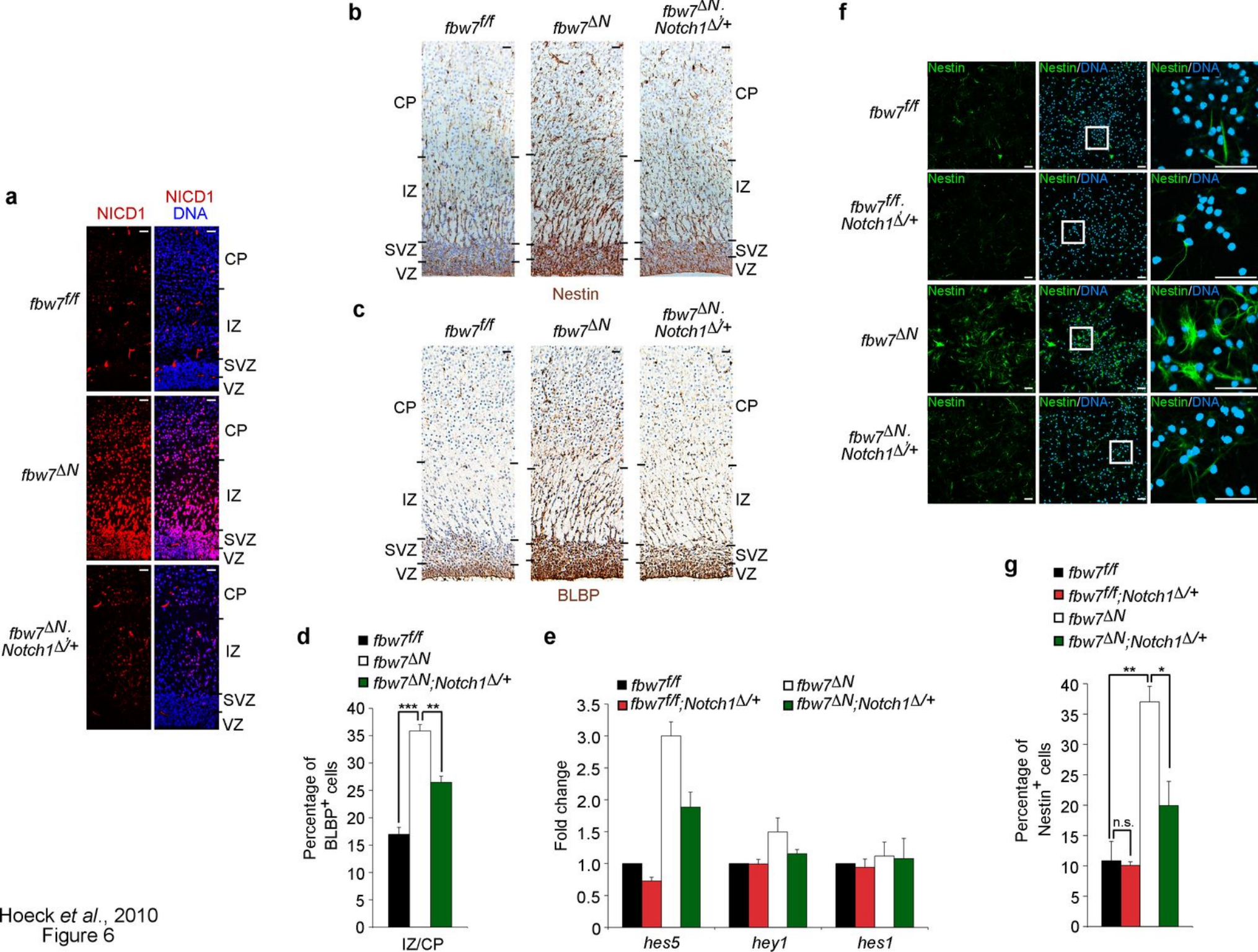


Hoeck *et al.*, 2010
Figure 6